Intravenous administration of iron dextran as a potential inducer for hemochromatosis: Development of an iron overload animal model

Erick Khristian[1,3], Mohammad Ghozali[2], Muhammad H. Bashari[2], Jeri N. Purnama[1], Gunawan Irianto[3], Ramdan Panigoro[2] and Ratu Safitri[4]*

[1]Doctoral Program in Biotechnology, Postgraduate School, Universitas Padjadjaran, Bandung, Indonesia; [2]Department of Biomedical Sciences, Faculty of Medicine, Universitas Padjadjaran, Bandung, Indonesia; [3]Faculty of Health Science and Technology, Universitas Jenderal Achmad Yani, Cimahi, Indonesia; [4]Department of Biology, Faculty of Mathematics and Natural Sciences, Universitas Padjadjaran, Jatinangor, Indonesia

*Corresponding author: ratu.safitri@unpad.ac.id

Abstract

Iron overload in transfusion-dependent thalassemia patients represents a significant public health challenge due to its high mortality rate and risks of severe complications. Therefore, developing safe and effective therapeutic modalities for managing iron overload is critical, as current animal models inadequately replicate human conditions. The aim of this study was to investigate the effects of intravenous iron dextran on hepatocyte morphology, liver iron concentration, and serum iron profile changes as a model for hemochromatosis. An experimental design with a post-test-only control group method was conducted using animal models. Fifty rats were used and divided into ten groups, nine received different intravenous doses of iron dextran: 10, 20, 30, 40, 50, 60, 80, 100, and 120 mg/kg body weight (BW) and a control group received no treatment. The results showed that intravenous iron dextran starting at a dose of 10 mg/kg BW caused significant changes in liver iron concentration while starting at 20 mg/kg BW significantly affected hepatocyte morphology, transferrin levels, unsaturated iron binding capacity, serum iron levels, and transferrin saturation. Intravenous iron dextran starting at 40 mg/kg BW resulted significant changes in the level of total iron binding capacity compared to control group. In conclusion, intravenous iron dextran significantly altered hepatocyte morphology, increased liver iron concentration, and modified the serum iron profile, reflecting changes that might be observed in patients with transfusion-dependent thalassemia.

Keywords: Thalassemia, iron dextran, iron overload, hepatocyte morphology, animal model

Introduction

*I*ron overload, particularly in transfusion-dependent thalassemia patients, pose a significant health concern with a high mortality rate if left untreated [1]. Elevated serum ferritin levels, particularly above 2000 μg/L, are strongly associated with severe complications, including cirrhosis, hepatocellular carcinoma, and metabolic dysfunctions [2]. Mortality rates are notably higher in patients with serum ferritin levels exceeding 2000 μg/L compared to those with levels below 1000 μg/L [3], underscoring the critical need for timely and effective management strategies for iron overload. A study found that 76% of transfusion-dependent thalassemia

patients had at least one comorbidity, with 40% having endocrine disorders, 40% osteoporosis, and 34% diabetes [4]. Additionally, heart disease was identified in 18% of patients, with atrial fibrillation and heart failure being the most prevalent, occurring in 11% and 9% of patients, respectively [4]. The mortality rate was recorded at 6.2%, significantly higher than the age- and sex-adjusted mortality rate in the general population (1.2%; $p<0.001$) [4], highlighting the need for comprehensive treatment, including iron chelation therapy, to reduce morbidity and improve survival in transfusion-dependent thalassemia patients [5].

Pharmacological and non-pharmacological therapies are used to manage iron overload [6]. Subcutaneous administration of deferoxamine, a common iron chelator, is associated with low adherence and various complications, including local reactions, ophthalmologic, auditory, pulmonary, and neurologic side effects [1,7]. In contrast, oral chelators such as deferiprone, although effective, it poses risks to agranulocytosis, liver fibrosis, renal toxicity, and infections [8,9].

Rodent models of iron overload using intraperitoneal or oral iron dextran have been established [10-14]. Intraperitoneal iron dextran administration has been shown to increase iron levels in test animals over a period of 4 to 12 weeks, with excess iron observed in the bone marrow, liver, kidneys, spleen, and serum iron parameters; however, certain parameters exhibit discrepancies when compared to transfusion-dependent thalassemia patients [15-18]. Studies utilizing oral administration of iron dextran as a negative control have also demonstrated iron overload, although the extent of organ iron accumulation did not reach the severe levels observed in transfusion-dependent thalassemia patients [13,14]. While these models are useful for studying iron overload pathophysiology and potential treatments, limitations exist, including long treatment durations, increased mortality, and induction pathways that do not fully mimic transfusion conditions [13-19]. The aim of this study was to investigate the effects of intravenous iron dextran on hepatocyte morphology, liver iron concentration, and serum iron profile changes, providing a more rapid and accurate hemochromatosis model that better reflects the iron overload conditions in transfusion-dependent thalassemia patients.

Methods

Study design and setting
A true experimental design with a post-test-only control group method was conducted to evaluate the effects of intravenous iron dextran on serum iron profiles, liver iron concentration, and hepatic histopathology, aiming to produce a hemochromatosis model in rats. Experimental procedures involving iron dextran administration were conducted at Faculty of Health Science and Technology, Universitas Jenderal Achmad Yani, Cimahi, Indonesia. Examinations of serum iron profiles, organ iron concentrations, and liver histopathology—utilizing hematoxylin-eosin and Prussian blue staining—were performed at the Department of Biomedical Sciences, Faculty of Medicine, Universitas Padjadjaran, Bandung, Indonesia.

The study commenced with the administration of iron dextran as an inducer of iron overload to Wistar strain rats (*Rattus norvegicus*) at varying doses and administration periods (**Table 1**). Fifty rats were employed and divided into ten groups, nine groups received nine different intravenous doses of iron dextran: 10, 20, 30, 40, 50, 60, 80, 100, and 120 mg/kg body weight (BW) and a control group that received no treatment. The test animals were euthanized 72 hours after the last injection after which blood and liver tissue samples were collected.

Sampling strategy and eligibility criteria
Healthy male rats were selected based on specific inclusion criteria: weights ranging from 150 to 180 grams, absence of physical defects such as broken tail, tilted heads, torn ears and skin wounds, with normal vision. Rats with body weights greater than ±20% and physical abnormalities such as the presence of wounds, blindness or impaired vision were excluded. Measurements to determine blindness and visual impairment were conducted using the maze method and an assessment of eye defects due to corneal dystrophy [20,21]. Federer formula was utilized to determine the required number of animals per group, resulting in a minimum sample size of three rats. To account for potential drop-out, an additional 50% was added, yielding a total

of five rats per group. Rats were allocated to experimental groups using conventional blind random sampling. This involved tagging the dorsal area of each rat with a secure, easily identifiable marker. Numbers corresponding to each rat were written on balls, which were then placed in a container. A blindfolded researcher randomly selected five balls to assign the rat numbers for group 1, and a similar procedure was followed for subsequent groups.

Animal preparation

Rats were housed in groups of five in well-shaded, tranquil rooms, with a consistent environment. Rats were provided with the same quantity and type of food, and a tray beneath each cage collected urine and feces, which were cleaned daily. Ventilated cages were maintained at a temperature of 25−27˚C and humidity of 50−60%. A 12:12 light-dark cycle was maintained, with lights on at 5:30 AM. Rats were fed formulated pellet feed at 10% of body weight, twice a day. Clean water was provided *ad libitum* through specialized bottles. The acclimatization period lasted for seven days.

Preparation of injection solution

Injection solution was prepared by diluting iron dextran in physiological saline. Physiological saline was created by dissolving 0.9 grams of sodium chloride (NaCl) (Sigma-Aldrich, Missouri, USA) in 100 mL of distilled deionized water (ddH$_2$O). Iron dextran (Sigma-Aldrich, Missouri, USA), initially at a concentration of 100 mg in 25 mL, was further diluted to prepare stock solutions of 10 mg/mL and 20 mg/mL for injection.

Iron dextran administration and collection of blood and liver

Different doses of iron dextran were administered intravenously via the lateral vein route in the tail as previously explained [22] and the amount of iron dextran according to the treatment groups (**Table 1**). The solution was prepared by diluting iron dextran in physiological saline to prepare stock solutions of 10 mg/mL and 20 mg/mL for injection. Each dose was delivered in a volume of up to 1 mL per 200 grams of body weight, with a maximum single injection of 20 mg/kg BW. Higher doses necessitated multiple injections; the injection location was done at a different point within the lateral vein. After 72 hours of the last iron dextran injection, the rats were anesthetized to obtain blood and followed by euthanasia to collect the liver; i.e., each group had a different euthanasia schedule (**Table 1**).

Rats were anesthetized with 10% ketamine hydrochloride (100 mg/kg BW, administered at the intraperitoneal in the lower right quadrant of the abdomen as recommended) [22]. Blood was collected from the rats via cardiac puncture of the right ventricle with the thoracic cavity opened [23]. The chest cavity was opened by cutting the sternum using a size 10 scalpel (Aesculap Scalpel Blades, Germany) with a 2×2 cm hole, until the heart was clearly visible. Whole blood was collected using a 26-gauge needle and a syringe volume of 5 mL (Terumo, Tokyo, Japan), then transferred into a 5 mL vacutainer tube containing separation gel (KBKI code: 3527002013, Indonesia) [24]. After obtaining blood samples, an additional 260 mg/kg BW ketamine was added with the total dose received being 360 mg/kg BW to ensure euthanasia at the time of hepatic collection [25]. Once the rat was confirmed deceased through the observation of cardiac arrest, a 4 cm longitudinal incision extending from the diaphragm and a 2 cm medial incision at the initial and final points of the incision, respectively, was performed using a number 10 scalpel. This resulted in the exposure of the abdominal cavity and the visualization of the liver. The liver was then harvested and thoroughly washed with saline solution. All sampling procedures were performed by laboratory personnel who are experts in rat dissection and blood collection.

Table 1. Iron dextran dosing scheme (mg/kg body weight (BW)) and administration schedule of iron dextran in study group

Groups	Day 0	Days 3	Days 6	Days 9	Days 12	Days 15
Control	-	-	-	-	-	-
Dose 10 mg/kg BW	10 mg/kg	-	-	-	-	-
Dose 20 mg/kg BW	20 mg/kg	-	-	-	-	-
Dose 30 mg/kg BW	20 mg/kg	10 mg/kg	-	-	-	-
Dose 40 mg/kg BW	20 mg/kg	20 mg/kg	-	-	-	-
Dose 50 mg/kg BW	20 mg/kg	20 mg/kg	10 mg/kg	-	-	-

Groups	Day 0	Days 3	Days 6	Days 9	Days 12	Days 15
Dose 60 mg/kg BW	20 mg/kg	20 mg/kg	20 mg/kg	-	-	-
Dose 80 mg/kg BW	20 mg/kg	20 mg/kg	20 mg/kg	20 mg/kg	-	-
Dose 100 mg/kg BW	20 mg/kg	20 mg/kg	20 mg/kg	20 mg/kg	20 mg/kg	-
Dose 120 mg/kg BW	20 mg/kg	20 mg/kg	20 mg/kg	20 mg/kg	20 mg/kg	20 mg/kg

Hepatocyte morphology measurement

Hepatic tissue was immersed in 10% neutral buffered formalin (Sigma-Aldrich, Missouri, USA) for 12 hours. The fixed tissue was then embedded in paraffin and processed using standard histology procedures [26] and were stained using hematoxylin-eosin (Merck & Co Inc, New Jersey, USA) and Prussian Blue (Sigma-Aldrich, Missouri, USA) for microscopic observation. Hematoxylin-eosin staining was employed to visualize alterations in hepatocyte morphology, while Prussian blue staining was utilized to assess the distribution of iron within the tissue.

Three independent pathologists evaluated ten fields of view (FOV) per sample, divided into four quadrants plus the center. Hepatocyte morphology (steatosis) was assessed using a semi-quantitative histopathology score based on non-alcoholic steatohepatitis (NASH) criteria. NASH scoring evaluates the severity of liver damage caused by iron dextran administration, which is the total score of the steatosis, lobular inflammation, and hepatocellular swelling scores [27]. Steatosis was characterized by the presence of intra-hepatocyte lipid droplets and evaluated using 40× microscopic magnification. Steatosis scoring was as follows: score 0 (less than 5% of hepatocytes show steatosis/FOV), score 1 (mild) (5% to 33% of hepatocytes show steatosis/FOV), score 2 (moderate) (34% to 66% of hepatocytes show steatosis/FOV), and score 3 (severe) (more than 66% of hepatocytes show steatosis/FOV). Lobular inflammation was assessed by counting inflammatory cell foci (e.g., lymphocytes and/or neutrophils) within the liver parenchyma at 200× magnification and the score was defined as follows: score 0 (no foci/FOV), score 1 (1 to 2 foci/FOV), score 2 (3 to 4 foci/FOV), and score 3 (more than 4 foci/FOV). Hepatocellular swelling indicated by enlarged hepatocytes with pale and irregular cytoplasm was assessed at 40× magnification with the following scores: score 0 (no swollen hepatocyte/FOV), score 1 (≤4 swollen hepatocytes/FOV), and score 2 (>4 swollen hepatocytes/FOV) [28]. Interpretation of scores for NASH diagnosis was as follows: a score of 0−2 is consistent with simple steatosis or non-alcoholic fatty liver disease without significant hepatocellular inflammation or swelling; a score of 3−4 suggests some inflammatory activity but is not definitive; and a score of ≥5 indicates significant steatosis, inflammation, and hepatocellular injury.

For Prussian blue staining, the tissue slides were observed at 400× magnification. Iron density/FOV was measured using ImageJ software (Wayne Rasband, Maryland, USA). Measurements with ImageJ software began with calibrating the density units to μm² using microscope slide calibration. The area of the iron density was measured in a FOV equalized by the microscope slide calibration with a size of 10×10 μm² [29].

Liver iron concentration measurement

Liver iron concentration was measured using flame atomic absorption spectrophotometry Spectrometer Analyst 400 (Perkin Elmer, Connecticut, USA) at Central Laboratory, Universitas Padjadjaran, Bandung, Indonesia. Briefly, 0.2 g of liver tissue was placed in a 25 mL beaker and treated with 5 mL of concentrated nitric acid (HNO_3), allowing it to stand at room temperature for 30 mins. Following the addition of 2 mL of 30% hydrogen peroxide (H_2O_2), the mixture was heated at 60°C until the solution became clear. An additional 5 mL of concentrated HNO_3 was then added, and the solution was analyzed using atomic absorption spectrophotometry at 248 nm as described previously [30]. Liver iron concentration, measured in parts per million (ppm), was converted to milligrams per gram of dry weight (mg/g DW) and categorized into four classifications: class 1 (<3 mg/g DW) for normal, class 2 (3−7 mg/g DW) for mild, class 3 (7−15 mg/g DW) for moderate, and class 4 (>15 mg/g DW) for severe iron overload [31].

Serum iron level measurements

The serum iron examination included measurements of unsaturated iron binding capacity (UIBC), serum iron (Fe), total iron binding capacity (TIBC), transferrin, and ferritin. UIBC, serum iron, and TIBC were assessed using spectrophotometry with Iron FS Ferene and UIBC FS kits (DiaSys Diagnostic Systems GmbH, Holzheim, Germany). A serum sample of 75 μL was utilized

for UIBC examination, measured at a wavelength of 623 nm. For serum iron analysis, 5 µL of serum was assessed at a wavelength of 596 nm. TIBC was calculated as the sum of UIBC and serum iron, with the results expressed in µg/dL. The transferrin saturation index was estimated using the formula of transferrin saturation index (%) equal to (serum iron/TIBC) ×100%. The normal reference ranges for UIBC, serum iron, TIBC, and transferrin saturation index are 120–470 µg/dL, 90–180 µg/dL, 250–450 µg/dL, and 15–50%, respectively [33].

Transferrin and ferritin levels were measured using the enzyme-linked immunoassay (ELISA) method with the Fine Test assay kit (Wuhan Fine Biological Technology, Wuhan, China). Each examination utilized a sample of 100 µL, and the procedure was performed according to the manufacturer's guidelines. All tests were measured at a wavelength of 450 nm using a Thermo Scientific Multiskan SkyHigh Microplate Spectrophotometer (Thermo Scientific, Singapore). The normal reference ranges for ferritin and transferrin are 30–360 µg/L [33] and 200–360 mg/dL [34], respectively.

Statistical analysis
Parametric data (liver iron concentration and serum iron profile) were analyzed using the ANOVA test to assess the differences among groups, followed by Bonferroni post-hoc test to compare the difference between control group and other groups. Non-parametric data (scores of steatosis, lobular inflammation, hepatocellular swelling and NASH and iron density) were tested using Kruskal-Wallis followed by the Mann-Whitney U test. Statistical analysis was performed with SPSS statistical software version 25.00 for windows (IBM, New York, USA), with a significance level of α=0.05.

Results

Effect of intravenous iron dextran on hepatocyte morphology
Varying degrees of steatosis were observed across groups, with the control group showing nearly undetectable steatosis levels in five visual fields. In contrast, groups treated with iron dextran exhibited significant increases in steatosis starting at a dose of 20 mg/kg BW. This trend corresponded with an increase in hepatocellular swelling. Focal inflammation, characterized by inflammatory cell aggregation, was evident in the group receiving 10 mg/kg BW of iron dextran and increased in both number and size at higher doses (**Figure 1**).
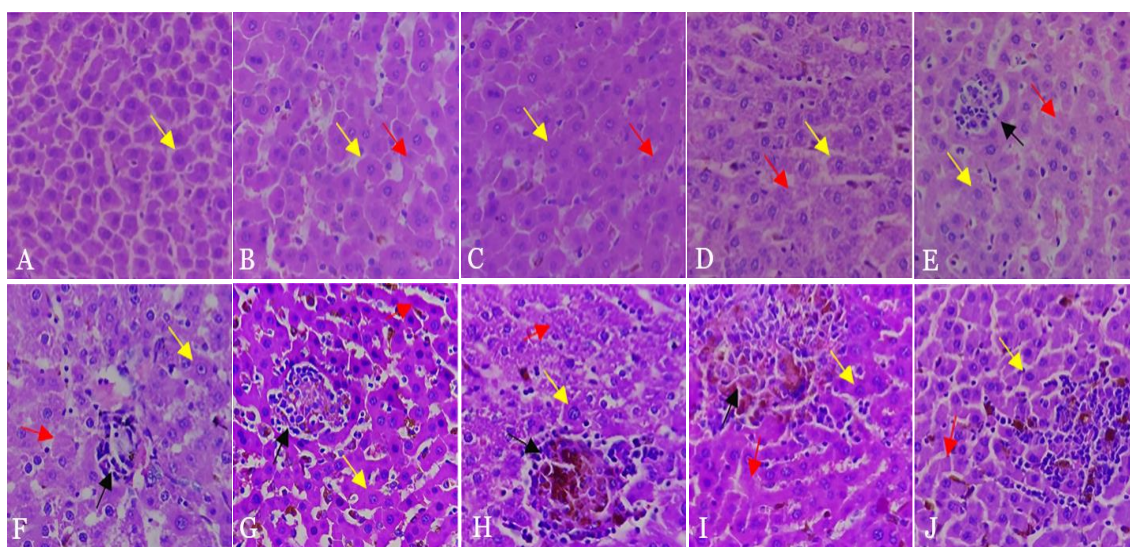
Figure 1. Hepatocyte morphology at 400× magnification with hematoxylin and eosin staining: control (A), 10 mg/kg BW (B), 20 mg/kg BW (C), 30 mg/kg BW (D), 40 mg/kg BW (E), 50 mg/kg BW (F), 60 mg/kg BW (G), 80 mg/kg BW (H), 100 mg/kg BW (I), and 120 mg/kg BW (J). Yellow arrows show normal cells, red arrows indicate necrotic cells, and black arrows mark foci.

Microscopic observations were analyzed using NASH score, the results showed that scores for steatosis, lobular inflammation, and hepatocyte swelling, as well as the overall NASH score,

increased gradually from an iron dextran dose of 10 mg/kg BW to 120 mg/kg BW. Steatosis and inflammation were significantly higher in animals within the 20 mg/kg BW group compared to the control group (with $p=0.016$ and $p=0.008$, respectively). Furthermore, hepatocyte swelling showed a significant increase at 30 mg/kg BW ($p=0.008$). The total NASH score was significantly different between the control group and treatment group stating the dose of 20 mg/kg BW ($p=0.008$), indicating that iron accumulation caused significant cellular damage (**Table 2**).

Table 2. Effect of intravenous iron dextran on scores of steatosis, lobular inflammation, hepatocellular swelling, and non-alcoholic steatohepatitis (NASH) score across groups

Study groups	Steatosis score	Lobular inflammation score	Swelling of hepatocyte score	NASH score
Control	0.04±0.89	0.04±0.09	0.04±0.09	0.12±0.17
Dose 10 mg/kg BW	0.20±0.14	0.32±0.23[*]	0.20±0.14	0.72±0.50
Dose 20 mg/kg BW	0.30±0.10[*]	0.50±0.10[*]	0.25±0.17[*]	1.06±0.36[*]
Dose 30 mg/kg BW	0.36±0.09[*]	0.27±0.10[*]	0.29±0.10[*]	0.92±0.23[*]
Dose 40 mg/kg BW	0.41±0.14[*]	0.46±0.17[*]	0.26±0.17[*]	1.14±0.24[*]
Dose 50 mg/kg BW	0.56±0.17[*]	0.55±0.17[*]	0.26±0.17[*]	1.36±0.43[*]
Dose 60 mg/kg BW	0.90±0.22[*]	0.70±0.10[*]	0.30±0.22[*]	1.90±0.46[*]
Dose 80 mg/kg BW	0.86±0.36[*]	0.66±0.26[*]	0.50±0.22[*]	2.02±0.74[*]
Dose 100 mg/kg BW	1.06±0.26[*]	0.96±0.38[*]	0.74±0.22[*]	2.76±0.78[*]
Dose 120 mg/kg BW	0.97±0.26[*]	0.97±0.17[*]	0.87±0.36[*]	2.80±0.76[*]

[*] Statistically significant at $p<0.05$, analyzed using Mann-Whitney test compared to control group

Effect of intravenous iron dextran on hepatic iron levels

Iron accumulation in the sinusoidal space was observed across all experimental groups treated with iron dextran. At a dosage of 10 mg/kg BW, the distribution of iron was negligible; however, as the dosage of iron dextran increased, the distribution became more extensive and pronounced. In the 120 mg/kg BW group, iron was present in both the sinusoidal area and hepatocyte cells, indicating significant hepatic iron accumulation due to iron dextran administration (**Figure 2**).
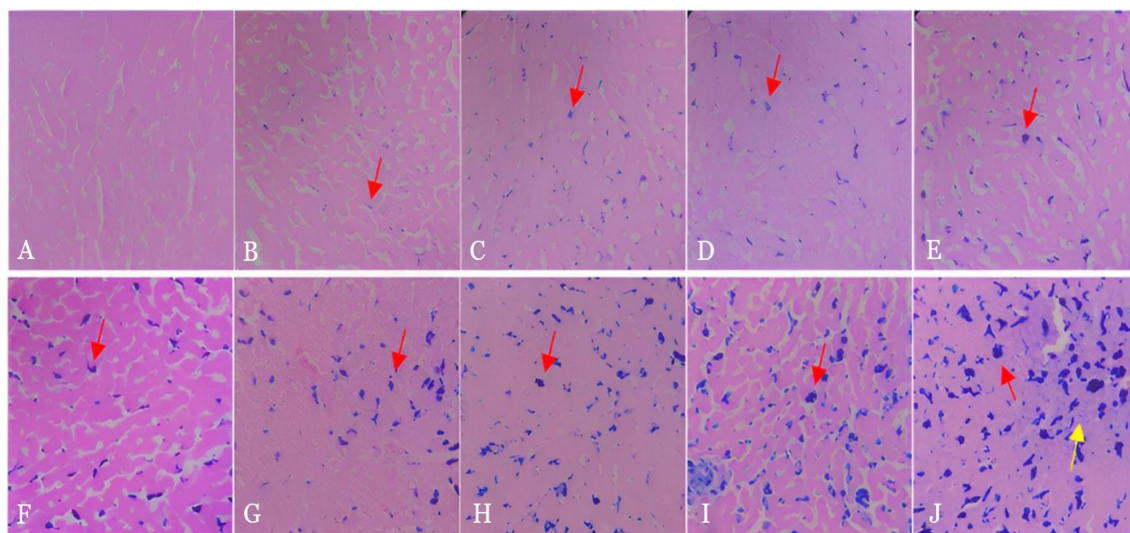
Figure 2. Liver tissue with Prussian blue staining at 400× magnification: control (A), 10 mg/kg BW (B), 20 mg/kg BW (C), 30 mg/kg BW (D), 40 mg/kg BW (E), 50 mg/kg BW (F), 60 mg/kg BW (G), 80 mg/kg BW (H), 100 mg/kg BW (I), 120 mg/kg BW (J). Red arrows show iron deposits (blue) and yellow arrows indicate iron in hepatocytes.

The average iron area and distribution percentage increased with the iron dextran dose. At a dosage of 10 mg/kg BW, the experimental group exhibited significantly elevated iron levels compared to the control group ($p=0.005$), with continued increases observed at higher doses, including 120 mg/kg BW (**Table 3**).

Measurement of iron levels using the atomic absorption spectrophotometry method revealed a statistically significant increase ($p<0.001$) based on the ANOVA test. Liver iron concentration values increased in accordance with the iron levels induced by dextran administration. In the

control group, liver iron concentration levels reflected the rat's endogenous metabolism. Hepatic tissue iron levels were averaged and classified to determine the degree of liver iron concentration [31].

Table 3. Comparisons of iron density per field of view (FOV) in hepatic tissue observed across study groups

Study groups	Iron density (µm²/FOV)	Percentage area (%)
Control	0	0
Dose 10 mg/kg BW	138[*]	0.14[*]
Dose 20 mg/kg BW	599[*]	0.62[*]
Dose 30 mg/kg BW	785[*]	0.81[*]
Dose 40 mg/kg BW	1028[*]	1.07[*]
Dose 50 mg/kg BW	1798[*]	1.87[*]
Dose 60 mg/kg BW	2297[*]	2.38[*]
Dose 80 mg/kg BW	3514[*]	3.65[*]
Dose 100 mg/kg BW	4309[*]	4.47[*]
Dose 120 mg/kg BW	8304[*]	8.61[*]

[*] Statistically significant at $p<0.05$, analyzed using Mann-Whitney test compared to the control group

Administration of iron dextran at a dosage of 10 mg/kg BW resulted in iron levels within the normal range (<3 mg Fe/g DW). Doses of 20 mg/kg BW to 40 mg/kg BW caused mild iron overload (3–7 mg Fe/g DW), while a dose of 50 mg/kg BW caused moderate iron overload (>7 mg Fe/g DW). Iron dextran with doses from 60 mg/kg BW to 120 mg/kg BW caused severe iron overload (>15 mg Fe/g DW) (**Table 4**). These findings indicated that iron dextran administration could elevate liver iron levels, a condition frequently observed in patients with thalassemia.

Table 4. Comparisons of liver iron concentration (LIC) measured across groups

Groups	Liver iron concentration (Fe/g dry weight)	Category based on liver iron concentration [31]
Control	0.25±0.03	Normal
Dose 10 mg/kg BW	2.56±0.21[*]	Normal
Dose 20 mg/kg BW	3.93±0.32[*]	Mild
Dose 30 mg/kg BW	4.47±0.11[*]	Mild
Dose 40 mg/kg BW	5.21±1.13[*]	Mild
Dose 50 mg/kg BW	14.37±1.52[*]	Moderate
Dose 60 mg/kg BW	18.94±0.75[*]	Severe
Dose 80 mg/kg BW	26.86±1.08[*]	Severe
Dose 100 mg/kg BW	30.20±0.87[*]	Severe
Dose 120 mg/kg BW	33.24±2.22[*]	Severe

[*] Statistically significant at $p<0.05$ compared to the normal group using Bonferroni test compared to the control group

Effect of intravenous iron dextran on serum iron profile

The serum iron profile revealed statistically significant changes across all parameters ($p<0.001$), as indicated by the ANOVA test (**Table 5**). Further analyses indicated that ferritin levels increased significantly from doses of 10 mg/kg BW to 120 mg/kg BW ($p<0.001$ for all groups) compared to the control group (**Table 5**). Similarly, serum iron concentrations rose significantly from doses of 20 mg/kg BW to 120 mg/kg BW ($p<0.001$ for all iron dextran-treated groups compared to control group) (**Table 5**). The increases were also observed in transferrin saturation percentages, beginning at a dose of 20 mg/kg BW (**Table 5**).

In contrast, there was a significant decline in UIBC starting at 20 mg/kg BW, with $p<0.001$ across all iron dextran-treated groups compared to the control group (**Table 5**). TIBC also significantly decreased at a dose of 40 mg/kg BW ($p=0.004$), with further reductions observed at doses starting from 50 mg/kg BW ($p<005$) (**Table 5**). Transferrin concentrations declined significantly beginning at 20 mg/kg BW ($p<0.05$) and from 30 mg/kg BW to 120 mg/kg BW ($p<0.001$) when compared to controls (**Table 5**). These results indicate that iron dextran administration significantly affected the iron profile, potentially leading to haemochromatosis-like conditions.

Table 5. Comparisons of serum iron profile across groups

Groups	Ferritin (µg/L)	Transferrin (mg/dL)	UIBC (µg/dL)	Serum iron (µg/dL)	TIBC (µg/dL)	Transferrin saturation (%)
Control	76.33±6.61	197.62 ±8.91	267.10±4.93	83.01± 5.79	350.20± 5.92	42.18±4.30
Dose 10 mg/kg BW	513.47±13.99[*]	192.33±6.86	254.0.2±10.95	84.84±3.78	338.84±11.19	44.17±2.79
Dose 20 mg/kg BW	515.01±10.90[*]	184.57±6.95[*]	227.56±18.99[*]	109.74±3.61[*]	336.31±0.73	59.5±2.20[*]
Dose 30 mg/kg BW	549.62±13.73[*]	176.71±2.40[*]	189.11±13.34[*]	156.62±4.13[*]	335.95±6.28	88.64±2.38[*]
Dose 40 mg/kg BW	616.48±32.75[*]	159.95±3.99[*]	165.95±1.22[*]	159.04±1.85[*]	324.99±14.72[*]	99.49±2.94[*]
Dose 50 mg/kg BW	725.21±52.37[*]	157.88±2.22 [*]	157.53±1.38[*]	170.98±6.89[*]	328.50±5.69[*]	108.29±4.24[*]
Dose 60 mg/kg BW	876.21±76.70[*]	151.66±5.25[*]	130.52±7.19[*]	187.18±3.96[*]	317.72±3.55[*]	123.54±4.80[*]
Dose 80 mg/kg BW	968.0±98.26[*]	123.40±0.51[*]	110.18±12.80[*]	205.58±10.26[*]	315.75±10.35[*]	166.58±7.70[*]
Dose 100 mg/kg BW	774.82±30.25[*]	113.98±2.19[*]	98.69±5.23[*]	208.94±8.17[*]	307.65±10.94[*]	183.35±7.77[*]
Dose 120 mg/kg BW	703.56±23.20[*]	105.13±4.11[*]	102.52±3.34[*]	209.96±5.51[*]	316.49±12.25[*]	200.14±13.32[*]

TIBC: total iron binding capacity; UIBC: unsaturated iron binding capacity
[*] Statistically significant at $p<0.05$, analyzed using Bonferroni test compared to the control group

Discussion

Elevated iron levels in patients with transfusion-dependent thalassemia, which can lead to elevated iron levels in the body, are associated with adverse effects on organ function, especially the liver. The damage is not only to the liver but can also occur in other organs, so this condition causes impaired mobility and increased motility in patients with transfusion-dependent thalassemia. The results of this study showed that intravenous iron dextran to rats at doses ranging from 10 mg/kg BW to 120 mg/kg BW resulted in microscopic damage to hepatocyte cells in the liver. In addition, this caused an increase in iron density in the liver, elevated liver iron concentration, and affected the serum iron profile, indicating that there was an increase in iron levels in the body.

Histopathologic evaluation in the present study revealed an increase in the NASH score starting from 20 mg/kg BW, indicating liver damage, particularly in lobular inflammation. Iron accumulation in the liver generates reactive oxygen species (ROS), leading to hepatocyte damage and increased inflammation [35]. Hepatic sinusoidal endothelial cells, which are highly active in endocytosis and express receptors to scavenge toxins, may be primarily affected, leading to liver injury [36]. Excess iron deposition produces ROS, which can damage nucleic acids, proteins, and lipids [37,38]. This ROS-induced damage results in lipid and protein peroxidation and reduction in liver antioxidants and nitric oxide, collectively harming hepatocytes [39]. Iron deposition-related liver damage is prominent in hereditary hemochromatosis, a genetic disorder affecting iron metabolism [40]. This condition leads to hepatocyte death, fibrosis, and ultimately liver cirrhosis and hepatocellular carcinoma [41,42].

The present study indicated a direct proportionality between iron dextran dose and liver iron concentration, demonstrating its effectiveness in inducing iron overload. Iron dextran initially accumulates in Kupffer cells, but with repeated administration, it was also stored in hepatocytes. Iron was observed within Kupffer cells at doses up to 100 mg/kg BW. However, at a dose of 120 mg/kg BW, iron was detected in hepatocytes, indicating that the administration of iron dextran does not predominantly target hepatocytes for infiltration. Iron in the sinusoidal area is predominantly located in Kupffer cells, which are specialized macrophages involved in iron metabolism [43]. The observed iron deposition pattern, characterized by accumulation in Kupffer cells and minimal hepatocellular iron, mirrors that seen in hematologic disorders such as thalassemia [44]. The present study confirms that varying doses and durations of iron administration effectively increase liver iron concentrations in experimental animals [44].

Liver iron concentration is the reference standard for assessing body iron stores and reliably predicts total iron content [45]. The present study found that intravenous iron dextran administration starting at 10 mg/kg BW significantly increased hepatic iron levels compared to controls. Iron dextran, although employed for the treatment of iron deficiency anemia, has been shown to induce iron overload in animal models [46]. The compound is taken up by macrophages through endocytosis, where it undergoes oxidation from Fe(2+) to Fe(3+) within the bloodstream [39]. Normal liver iron concentration ranges vary; values below 3 mg/g DW are considered normal, while values above 7 mg/g DW indicate moderate iron overload, with risks increasing significantly at levels above 15 mg/g DW, and for patients with hereditary hemochromatosis, liver iron concentration can exceed 20 mg/g DW [19,20].

Serum iron profile measurements in the present study showed increased levels of serum iron, ferritin, and transferrin saturation, indicating iron overload. Although studies specifically using iron dextran in rat models of hemochromatosis are lacking, existing studies support that elevated serum iron, ferritin, and transferrin saturation are markers of iron overload [49-51]. Elevated transferrin saturation (>55%) is particularly useful for diagnosing hereditary hemochromatosis, while serum ferritin is valuable for assessing the need for and response to venesection [52,53].

The findings of the present study align with those reported previously, demonstrating that elevated liver iron levels correlate with increased ferritin levels due to the inflammatory response and liver damage induced by injected iron dextran [54]. The present study further supports prior research suggesting that increased ferritin levels are associated with liver damage and may signify pathological iron metabolism [55]. Furthermore, the observed increase in serum iron can be

attributed to hepatic injury caused by iron dextran, as evidenced by Milic *et al.*, who reported a correlation between hepatic injury and increased serum iron levels [56].

In the present study, the decrease in TIBC and transferrin levels suggested hemochromatosis [49,57,58]. TIBC is the primary diagnostic test for iron deficiency anemia and other iron metabolism disorders, reflecting the capacity of transferrin to bind iron, and when iron stores are depleted, transferrin levels increase [57]. This is consistent with a previous study showing that administering iron dextran to test animals resulted in elevated serum iron levels and decreased TIBC, thereby increasing transferrin saturation [59].

In this study, the developed hemochromatosis model was primarily examined through serological and histological indicators. However, in patients with thalassemia who develop hemochromatosis, the underlying causes may involve erythrocyte destruction or alternative pathways of iron uptake. Advancing this model of hemochromatosis could lead to innovative treatment options for patients with iron overload conditions, including those with transfusion-dependent thalassemia and other etiologies.

Conclusion

Intravenous iron dextran significantly altered hepatocyte morphology, increased liver iron concentration, and modified the serum iron profile, reflecting changes observed in patients with transfusion-dependent thalassemia. Therefore, this model can be used as a hemochromatosis model that better reflects the iron overload conditions in transfusion-dependent thalassemia patients.

Ethics approval

Protocol of the present study was reviewed and approved by Ethical Committee for Animal Research, Universitas Padjadjaran, Bandung, Indonesia (Approval number: 75/UN6.KEP/EC/2023).

Acknowledgments

The authors express gratitude to the staff of Central Laboratory, Universitas Padjadjaran, Bandung, Indonesia.

Competing interests

All the authors declare that there are no conflicts of interest.

Funding

How to cite

Khristian E, Ghozali M, Bashari MH, *et al.* Intravenous administration of iron dextran as a potential inducer for hemochromatosis: Development of an iron overload animal model. Narra J 2024; 4 (3): e1003 - http://doi.org/10.52225/narra.v4i3.1003.

References

1. Italia K, Colah R, Ghosh K. Experimental animal model to study iron overload and iron chelation and review of other such models. Blood Cells Mol Dis 2015;55(3):194-199.

2. Porter JL, Rawla P. Hemochromatosis. Med Interna Mex 2021;35(6):896-905.

3. McDowell LA, Kudaravalli P, Chen RJ, Sticco KL. Iron overload. In: Akcley WB, Adolphe TS, Aeby TC, *et al.*, editors. StatPearls. Treasure Island (FL): StatPearls Publishing; 2024.

4. Tuo Y, Li Y, Li Y, *et al.* Global, regional, and national burden of thalassemia, 1990–2021: A systematic analysis for the global burden of disease study 2021. EClinicalMedicine 2024;72:102619.

5. Mariani D, Rochimat I. Kebutuhan self management bagi penyandang thalassemia. Med Inform 2023;19(1):116-121.

6. Lima TG de, Benevides FLN, Esmeraldo Filho FL, *et al*. Treatment of iron overload syndrome: A general review. Rev Assoc Med Bras 2019;65(9):1216-1222.

7. Entezari S, Haghi SM, Norouzkhani N, *et al*. Iron chelators in treatment of iron overload. J Toxicol 2022;2022:1-18.

8. Rindarwati AY, Diantini A, Lestari K. Efficacy and side effects of deferasirox and deferiprone for thalasemia major in children. Pharmacol Clin Pharm Res 2016;1(3):74-78.

9. Hruby M, Martínez IIS, Stephan H, *et al*. Chelators for treatment of iron and copper overload: Shift from low-molecular-weight compounds to polymers. Polym 2021;13(22):3969.

10. Jahanshahi M, Khalili M, Margedari A. Naringin chelates excessive iron and prevents the formation of amyloid-beta plaques in the hippocampus of iron-overloaded mice. Front Pharmacol 2021;12:651156.

11. Chan LSA, Gu LCH, Wells RA. The effects of secondary iron overload and iron chelation on a radiation-induced acute myeloid leukemia mouse model. BMC Cancer 2021;21(1):509.

12. Martin D, Nay K, Robin F, *et al*. Oxidative and glycolytic skeletal muscles deploy protective mechanisms to avoid atrophy under pathophysiological iron overload. J Cachexia Sarcopenia Muscle 2022;13(2):1250-1261.

13. Maskoen AM, Safitri R, Milanda T, *et al*. Iron chelation ability of Granule sappan wood (*Caesalpinia sappan* L.) extract on iron-overloaded. Int J PharmTech Res 2016;9(5):299-305.

14. Safitri R, Maskoen AM, Syamsunarno MRAA, *et al*. Iron chelating activity of *Caesalpinia sappan* L. extract on iron status in iron overload rats (*Rattus norvegicus* L.). AIP Conf Proc 2018;2002(1):020050.

15. Sheikh NA, Desai TR, Tirgar PR. Evaluation of iron chelating and antioxidant potential of *Epilobium hirsutum* for the management of iron overload disease. Biomed Pharmacother 2017;89:1353-1361.

16. Odeh D, Oršolić N, Adrović E, *et al*. The Impact of the combined effect of inhalation anesthetics and iron dextran on rats' systemic toxicity. Int J Mol Sci 2024;25(12):6323.

17. Adham KG, Farhood MH, Daghestani MH, *et al*. Metabolic response to subacute and subchronic iron overload in a rat model. Acta Biol Hung 2015;66(4):361-373.

18. Tian C, Zhao J, Xiong Q, *et al*. Secondary iron overload induces chronic pancreatitis and ferroptosis of acinar cells in mice. Int J Mol Med 2023;51(1):9.

19. Zhang Y, Zhai W, Zhao M, *et al*. Effects of iron overload on the bone marrow microenvironment in mice. PLoS One 2015;10(3):e0120219.

20. Monk C. Ocular surface disease in rodents (guinea pigs, mice, rats, chinchillas). Vet Clin North Am Exot Anim Pract 2019;22(1):15-26.

21. Leinonen H, Tanila H. Vision in laboratory rodents–Tools to measure it and implications for behavioral research. Behav Brain Res 2018;352:172-182.

22. Fukuta K. Collection of body fluids. In: Hedrich HJ, Bullock G, editors. The laboratory mouse. Amsterdam: Elsevier; 2004.

23. Goutianos G, Margaritelis N V., Sparopoulou T, *et al*. Chronic administration of plasma from exercised rats to sedentary rats does not induce redox and metabolic adaptations. J Physiol Sci 2020;70(1):1-10.

24. Parasuraman S, Raveendran R, Kesavan R. Erratum: Blood sample collection in small laboratory animals. J Pharmacol Pharmacother 2017;8(3):153.

25. AVMA. AVMA guidelines for the euthanasia of animals: 2020 edition. Available from: https://www.avma.org/sites/default/files/2020-02/Guidelines-on-Euthanasia-2020.pdf. Accessed: 23 Oct. 2024.

26. Khristian E, Inderiati D. Sitohistoteknologi. Jakarta: Kementerian Kesehatan Republik Indonesia; 2017.

27. Pappachan J, Babu S, Krishnan B, Ravindran NC. Non-alcoholic fatty liver disease: A clinical update. J Clin Transl Hepatol 2017;5(4):384-393.

28. Gill RM, Allende D, Belt PH, *et al*. The nonalcoholic steatohepatitis extended hepatocyte ballooning score: Histologic classification and clinical significance. Hepatol Commun 2023;7(2):e0033.

29. Rosa G de AA, De Araújo MF, Aguiar LS, *et al*. Computerized morphometry of the area of the hard palate and of palatal rugae: A cross-sectional study. Med Leg Costa Rica 2020;37(1):154-161.

30. Wortmann AC, Froehlich PE, Pinto RB, *et al*. Hepatic iron quantification by atomic absorption spectrophotometry: Full validation of an analytical method using a fast sample preparation. J Spectrosc 2007;21(3):761029.

31. Taher AT, Musallam KM, Hoffbrand AV. Current Strategies in the assessment of iron overload. EJCMO 2010;3:30-37.

32. Kanbour I, Chandra P, Soliman A, *et al*. Severe liver iron concentrations (LIC) in 24 patients with β-thalassemia major: Correlations with serum ferritin, liver enzymes and endocrine complications. Mediterr J Hematol Infect Dis 2018;10(1):e2018062.

Short Communication

33. DePalma RG, Hayes VW, O'Leary TJ. Optimal serum ferritin level range: Iron status measure and inflammatory biomarker. Metallomics 2021;13(6):mfab030.

34. Ogun AS, Adeyinka A. Biochemistry, Transferrin. In: Akcley WB, Adolphe TS, Aeby TC, *et al.*, editors. StatPearls. Treasure Island (FL): StatPearls Publishing; 2024.

35. Miyanishi K, Tanaka S, Sakamoto H, Kato J. The role of iron in hepatic inflammation and hepatocellular carcinoma. Free Radic Biol Med 2019;133:200-205.

36. Patten DA, Wilkinson AL, O'Keeffe A, Shetty S. Scavenger receptors: Novel roles in the pathogenesis of liver inflammation and cancer. Semin Liver Dis 2022;42(1):e1.

37. Aranda-Rivera AK, Cruz-Gregorio A, Arancibia-Hernández YL, *et al.* RONS and oxidative stress: An overview of basic concepts. Oxygen 2022;2(4):437-478.

38. Juan CA, Pérez de la Lastra JM, Plou FJ, Pérez-Lebeña E. The chemistry of reactive oxygen species (ROS) revisited: Outlining their role in biological macromolecules (DNA, lipids and proteins) and induced pathologies. Int J Mol Sci 2021;22(9):4642.

39. Galaris D, Barbouti A, Pantopoulos K. Iron homeostasis and oxidative stress: An intimate relationship. Biochim Biophys Acta Mol Cell Res 2019;1866(12):118535.

40. Piperno A, Pelucchi S, Mariani R. Inherited iron overload disorders. Transl Gastroenterol Hepatol 2020;5:25.

41. Handa P, Vemulakonda AL, Maliken BD, *et al.* Differences in hepatic expression of iron, inflammation and stress-related genes in patients with nonalcoholic steatohepatitis. Ann Hepatol. 2017;16(1):77-85.

42. Bloomer SA, Brown KE. Iron-induced liver injury: A critical reappraisal. Int J Mol Sci 2019;20(9):2132.

43. Mertens C, Marques O, Horvat NK, *et al.* The macrophage iron signature in health and disease. Int J Mol Sci 2021;22(16):8457.

44. Salomao MA. Pathology of hepatic iron overload. Clin Liver Dis (Haboken) 2021;17(4):232-237.

45. Angelucci E, Brittenham GM, McLaren CE, *et al.* Hepatic iron concentration and total body iron stores in thalassemia major. N Engl J Med 2000;343(5):327-331.

46. Latunde-Dada GO, McKie AT, Simpson RJ. Animal models with enhanced erythropoiesis and iron absorption. Biochim Biophys Acta 2006;1762(4):414-423.

47. Reeder SB, Yokoo T, França M, *et al.* Quantification of liver iron overload with MRI: Review and guidelines from the ESGAR and SAR. Radiology 2023;307(1):e221856.

48. Wood JC. Guidelines for quantifying iron overload. Hematology Am Soc Hematol Educ Program 2014;2014(1):210-215.

49. Ganz T. Iron metabolism. In: Kaushansky K, Lichtman MA, Prchal JT, *et al.*, editors. Williams hematology, 9e. New York, NY: McGraw-Hill Education; 2015.

50. Ministry of Health New Zealand. Iron overload (haemochromatosis). Available from: https://info.health.nz/conditions-treatments/blood/iron-overload-haemochromatosis. Accessed: 6 Jun. 2022.

51. Godbold M, McFarland PD. Iron overload. In: Scher CS, Kaye AD, Liu H, *et al.*, editors. Essentials of blood product management in anesthesia practice.Cham: Springer Cham; 2022.

52. Lands R, Isang E. Secondary hemochromatosis due to chronic oral iron supplementation. Case Rep Hematol 2017;2017:249416.

53. Wu LY, Song ZY, Li QH, *et al.* Iron chelators reverse organ damage in type 4B hereditary hemochromatosis: Case reports. Medicine (Baltimore) 2021;100(13):e25258.

54. Majd Z, Haghpanah S, Ajami GH, *et al.* Serum ferritin levels correlation with heart and liver MRI and LIC in patients with transfusion-dependent thalassemia. Iran Red Crescent Med J 2015;17(4):e24959.

55. Chen H. Iron metabolism in non-alcoholic fatty liver disease: A promising therapeutic target. Liver Res 2022;6(4):203-213.

56. Milic S, Mikolasevic I, Orlic L, *et al.* The role of iron and iron overload in chronic liver disease. Med Sci Monit 2016;22:2144-2151.

57. Faruqi A, Zubair M, Mukkamalla SKR. Iron Binding Capacity. In: Akcley WB, Adolphe TS, Aeby TC, *et al.*, editors. StatPearls. Treasure Island (FL): StatPearls Publishing; 2024.

58. Shander A, Cappellini MD, Goodnough LT. Iron overload and toxicity: The hidden risk of multiple blood transfusions. Vox Sang 2009;97(3):185-197.

59. Garcia-Casal MN, Pasricha SR, Martinez RX, *et al.* Serum or plasma ferritin concentration as an index of iron deficiency and overload. Cochrane Database Syst Rev 2021;5(5):CD011817.